Pure and Applied Mathematics Journal
2023; 12(4): 59-71
http://www.sciencepublishinggroup.com/j/pamj
doi: 10.11648/j.pamj.20231204.11
ISSN: 2326-9790 (Print); ISSN: 2326-9812 (Online)

Predator-Prey Interactions: Insights into Allee Effect Subject to Ricker Model

M. Y. Hamada[1, 2, *], Tamer El-Azab[1], H. El-Metwally[1]

[1]Mathematics Department, Faculty of Science, Mansoura University, Mansoura, Egypt
[2]Mathematics Department, Faculty of Engineering, German International University, Cairo, Egypt

Email address:
moe_hamada87@hotmail.com (M. Y. Hamada), Tamerazab@mans.edu.eg (Tamer El-Azab), helmetwally@mans.edu.eg (H. El-Metwally)
*Corresponding author

To cite this article:
M. Y. Hamada, Tamer El-Azab, H. El-Metwally. Predator-Prey Interactions: Insights into Allee Effect Subject to Ricker Model. *Pure and Applied Mathematics Journal*. Vol. 12, No. 4, 2023, pp. 59-71. doi: 10.11648/j.pamj.20231204.11

Received: May 16, 2023; **Accepted:** July 19, 2023; **Published:** September 25, 2023

Abstract: This study investigates the dynamic properties of a discrete predator-prey model influenced by the Allee effect. Through rigorous analysis utilizing bifurcation theory and the center manifold theorem, we establish the stability of the system's local equilibrium and reveal the intricate dynamical behaviors exhibited by the model, including period-doubling bifurcations at periods 2, 4, and 8, as well as the emergence of quasi-periodic orbits and chaotic sets. A notable finding is the significant role played by the parameter r in shaping the system's behavior, as we identify a series of bifurcations, such as flip and Neimark-Sacker bifurcations, by systematically varying r while keeping other parameters fixed. These findings underscore the non-linear nature of the model and provide valuable insights into its complex dynamics. Our enhanced understanding of these bifurcations and resulting dynamical behaviors deepens our knowledge of the Allee effect's implications for predator-prey models, contributing to our comprehension of population oscillations, stability transitions, and the emergence of chaotic dynamics in ecological systems under the Allee effect. Moreover, this study carries practical implications for population management and conservation strategies, as incorporating the Allee effect into predator-prey interactions allows for better insights into population dynamics and the development of more effective and sustainable management practices. Overall, this comprehensive analysis of the discrete predator-prey model under the Allee effect uncovers intricate dynamical behaviors and emphasizes the influential role of the parameter r in shaping system dynamics, with implications for both theoretical understanding and practical conservation management strategies.

Keywords: Discrete Predator-prey System, Allee Effect, Stability Analysis, Bifurcation Theory

1. Introduction

Population dynamics is a fundamental field of research in mathematical biology that examines how populations of species change over time. The study of population dynamics has a wide range of applications, including wildlife conservation, resource management, and epidemiology [1].

There are two primary mathematical models used in population dynamics research: continuous−time models, which are described by differential equations, and discrete−time models, which are described by difference equations. Continuous−time models are widely used and have been studied extensively for many years. However, discrete−time models have received increasing attention in recent years due to their ability to better capture the behavior of populations with non−overlapping generations or minimal population numbers, which are not accurately modeled by continuous−time models [2, 3].

In addition, discrete−time models are beneficial in producing more precise numerical simulation results. Discretization is often used to produce numerical simulations of continuous−time models, but this process can introduce errors that impact the accuracy of the results. Discrete−time models can overcome this issue by directly representing the population dynamics through difference equations.

Furthermore, discrete−time models can exhibit more complex and sophisticated dynamical behaviors than continuous−time models, such as bifurcations, chaos, and other complicated dynamics [4]. These dynamical behaviors have been the subject of much research and have yielded valuable insights into the behavior of populations in response to different ecological conditions.

Many authors have extensively investigated the stability, permanence, and existence of periodic solutions of predator−prey models [5–19]. However, research on the dynamical characteristics of predator−prey models, such as bifurcations and chaos occurrences in discrete−time models, has been limited.

Furthermore, there is a lack of research on the stability of discrete predator−prey systems with Allee effect. The Allee effect is a biological phenomenon that describes a positive relationship between population density and the rate of per capita growth, named after Allee [20]. This means that individual reproduction and survival are reduced at lower population densities, while this impact typically saturates or vanishes as populations grow larger. Various factors could cause this impact, including the difficulty in finding a mate for reproduction in some species when population density drops. Recently, there have been a few studies on the Allee effect in discrete predator−prey systems. For instance, Ye et al [21] analyzed a discrete−time predator−prey model with Allee effect and demonstrated the existence of a global attractor with a stable equilibrium point. Moreover, METWALLY et al [22] investigated the existence of chaotic dynamics in a discrete predator−prey system with Allee effect. This study revealed the coexistence of multiple attractors and chaos occurrence through a bifurcation analysis. Therefore, while many studies have examined predator−prey models, more research is necessary to explore the dynamical characteristics and stability of discrete predator−prey systems with Allee effect.

The difference equations presented below are utilized to define a discrete−time predator−prey model with Allee effect

$$\begin{aligned} x_{n+1} &= x_n\Big(r\mathrm{e}^{(1-x_n)}\big(x_n-\mu\big)-\delta y_n\Big), \\ y_{n+1} &= y_n\left(\alpha x_n-\gamma\right). \end{aligned} \tag{1}$$

The model components can be interpreted as follows:

1. The term $rx_n\mathrm{e}^{(1-x_n)}$ represents the growth of prey population according to the Ricker model when predators are absent. The term $x_n-\mu$ represents the Allee effect, which describes the positive relationship between population density and the rate of per capita growth.
2. $\delta x_n y_n$ represents the decrease in prey population due to predation by the predators.
3. $\alpha x_n y_n$ represents the increase in predator population as a function of the prey population.
4. γy_n represents the natural death rate of the predator population.

The objective of this study is to explore the implications of substituting the Ricker model, $rx_n\mathrm{e}^{(1-x_n)}$, for the conventional logistic growth term, $rx_n(1-x_n)$, in predator-prey models. Additionally, we aim to examine the influence of applying the Allee effect to this discrete predator-prey system.

The paper is structured as follows: In the second and third sections, we discuss the existence and local stability of equilibria in model (1). The fourth section examines the flip bifurcation and Neimark-Sacker bifurcation of model (1) by utilizing r as a bifurcation parameter. In the fifth section, we provide numerical simulations that not only demonstrate our theoretical results but also showcase complex dynamic behaviors, including a cascade of period-doubling bifurcation in periods 2, 4, and 8, as well as quasi-periodic orbits and chaotic sets. Finally, we present our discussion in the last section.

2. Stability Analysis

Our analysis begins with an examination of the equilibria in model (1). As expected, the point $E_0=(0,0)$ is one such equilibrium. Moreover, we can deduce that the remaining equilibria of model (1) fulfill the subsequent requirements:

$$\begin{aligned} r(x\mu)\mathrm{e}^{1-x}-\delta y-1&=0, \\ \alpha x-\gamma-1&=0. \end{aligned} \tag{2}$$

Solving System (2) allows us to find the other equilibrium point, which is

$$E_2=\left(\frac{\gamma+1}{\alpha},-\frac{r(\alpha\mu-\gamma-1)\mathrm{e}^{\frac{\alpha-\gamma-1}{\alpha}}+\alpha}{\delta\alpha}\right).$$

The equilibrium point E_2 is considered positive if

$$\gamma+1-\alpha\mu>\frac{\alpha}{r}\mathrm{e}^{\frac{\gamma-\alpha+1}{\alpha}}.$$

Another equilibrium point, $E_1(x^*,0)$, exists at the boundary and can be described by the equation $r(x^*-\mu)\mathrm{e}^{1-x^*}=1$. To find E_1, define the function $g(x)=r(x-\mu)\mathrm{e}^{1-x}-1$. We note that $g(0)=-\mu r\mathrm{e}-1<0$, $\lim_{x\to\infty}g(x)=-1$, and $g^{'}(x)=r(1-x+\mu)\mathrm{e}^{1-x}$. Hence, $g(x)$ has a unique equilibrium point at $x=1+\mu$. Thus, we can identify the following three cases:

1. If $r<\mathrm{e}^{\mu}$, there are no positive roots for $g(x)$.
2. If $r=\mathrm{e}^{\mu}$, $g(x)$ possesses a single positive root, which can be found at $x=1+\mu$. Therefore, we can identify E_1 as $(1+\mu,0)$.
3. When $r>\mathrm{e}^{\mu}$, $g(x)$ has two positive roots, specifically $x_1^*<1+\mu$ and $x_2^*>1+\mu$. We can refer to the corresponding equilibrium points of model (1) as $E_{11}=(x_1^*,0)$ and $E_{12}=(x_2^*,0)$.

3. Linearized Stability

This section presents the local stability conditions for the equilibrium points of the model. By computing the variation matrix corresponding to each equilibrium point, we can analyze the model's local stability. The Jacobian matrix J of model (1) evaluated at (x, y) is used to obtain this variation matrix.

$$J = \begin{pmatrix} \big(-x^2+(\mu+2)x-\mu\big)re^{1-x}-\delta y & -\delta x \\ \alpha y & \alpha x-\gamma \end{pmatrix},$$

We can obtain the characteristic equation of the Jacobian matrix as follows:

$$\sigma^2 - p(x,y)\sigma + q(x,y) = 0, \tag{3}$$

where

$$p(x,y) = \left(-x^2+(\mu+2)x-\mu\right)re^{1-x} - \delta y + \alpha x - \gamma,$$
$$q(x,y) = (\alpha x-\gamma)r\left(-x^2+(\mu+2)x-\mu\right)e^{1-x} + \delta\gamma y.$$

Proposition 3.1. The following statements are true for the equilibrium point E_0 of System (1):

(i) If $0 < r\mu < e^{-1}$ and $0 < \gamma < 1$, then E_0 is locally asymptotically stable, or a sink point.
(ii) If $r\mu > e^{-1}$ and $\gamma > 1$, then E_0 is an unstable source.
(iii) If $r\mu < e^{-1}$ and $\gamma > 1$, or if $r\mu > e^{-1}$ and $\gamma < 1$, then E_0 is an unstable saddle.
(iv) If $r\mu = e^{-1}$, or if $\gamma = 1$, then E_0 is a non-hyperbolic equilibrium.

Proof: The eigenvalues of the Jacobian matrix evaluated at E_0 are $\sigma_1 = -r\mu e$ and $\sigma_2 = -\gamma$. Thus the results of this Proposition can be obtain by comparing the position of the eigenvalues with respect to the unit circle. □

One of the eigenvalues of the equilibrium $E_0(0,0)$ is observed to be 1, according to Proposition (3.1). Therefore, a perturbed values of the parameters about $r\mu = e^{-1}$ or $\gamma = 1$ can result in a fold bifurcation of the system.

Proposition 3.2. The equilibrium point E_0 of the System (1) exhibits global asymptotic stability if and only if $0 < r\mu < e^{-1}$ and $0 < \gamma < 1$.

Proof: Proposition 3.1 established that E_0 is locally asymptotically stable when $0 < r\mu < e^{-1}$ and $0 < \gamma < 1$. Therefore, demonstrating that $\lim_{n\to\infty} x_n = 0$ and $\lim_{n\to\infty} y_n = 0$ is sufficient to establish the global stability of E_0.

$$\begin{aligned} x_{n+1} &= x_n\Big(re^{(1-x_n)}\big(x_n-\mu\big) - \delta y_n\Big), \\ &= r(x_n)^2e^{(1-x_n)} - r\mu x_n e^{(1-x_n)} - \delta x_n y_n, \\ &\le rex_n(x_n e^{(-x_n)}), \\ &\le rex_n. \end{aligned}$$

Hence

$$x_n \le (re)^n x_0, \quad n = 1, 2, \ldots \tag{4}$$

Thus

$$\lim_{n\to\infty} x_n = 0.$$

Noting that

$$\begin{aligned} 0 \le x_{n+1} &\iff 0 \le x_n\Big(re^{(1-x_n)}\big(x_n-\mu\big) - \delta y_n\Big), \\ &\iff \delta y_n \le ree^{(-x_n)}\big(x_n-\mu\big) \le ree^{(-x_n)}\big(x_n\big), \\ &\iff y_n \le \frac{re}{\delta}. \end{aligned}$$

Therefore, we can conclude that y_n is bounded from above. Examining the second equation of System (1) and equation (4), we obtain:

$$\begin{aligned} y_{n+1} = \alpha x_n y_n - \gamma y_n &\le \alpha x_n y_n \\ &\le \alpha(re)^n x_0 y_n \\ &\le \frac{\alpha}{\delta}(re)^{n+1}x_0, \quad n = 1, 2, \ldots. \end{aligned}$$

Therefore

$$\lim_{n\to\infty} y_n = 0.$$

Then the proof is completed. □

Proposition 3.3. The equilibrium point of System (1), $E_1(1+\mu, 0)$, is always non-hyperbolic.

Proof: The eigenvalues of $J(E_1)$ are $\sigma_1 = 1$ and $\sigma_2 = \alpha(1+\mu) - \gamma$.
Thus, we can conclude that the proof is complete. □

Proposition 3.4. The equilibrium points $E_{1i}(x_i^*, 0)$ of System (1), where $i \in \{1, 2\}$, satisfies the following statements:

(i) If $|\alpha x_i^* - \gamma| < 1$ and $|x_i^*(re^{1-x_i^*} - 1) + 1| < 1$, then E_{1i} is a sink point;
(ii) If $|\alpha x_i^* - \gamma| > 1$ and $|x_i^*(re^{1-x_i^*} - 1) + 1| > 1$, then E_{1i} is a source;
(iii) If $|\alpha x_i^* - \gamma| > 1$ and $|x_i^*(re^{1-x_i^*} - 1) + 1| < 1$, or if $|\alpha x_i^* - \gamma| < 1$ and $|x_i^*(re^{1-x_i^*} - 1) + 1| > 1$, then E_{1i} is a saddle;
(iv) If $|\alpha x_i^* - \gamma| = 1$, or if $|x_i^*(re^{1-x_i^*} - 1) + 1| = 1$, then E_{1i} is non-hyperbolic;

Proof: The outcomes of this Proposition can be obtained by noticing that the eigenvalues of $J(E_{1i})$ are $\sigma_1 = \alpha x_i^* - \gamma$ and $\sigma_2 = x_i^*(re^{1-x_i^*} - 1) + 1$. □

Proposition 3.5. If the following conditions are satisfied, the positive equilibrium point E_2 of model (1) is locally asymptotically stable:

(i) $\alpha^2\mu - (2\mu+\gamma+3)\alpha + 2\alpha + 2 < \frac{\alpha^2(3-\gamma)}{\gamma+1}e^{\frac{1+\gamma-\alpha}{\alpha}}$;
(ii) $\alpha^2\mu - (\mu+\gamma+2)\alpha + \gamma + 1 < \frac{-\alpha^2}{r}e^{\frac{1+\gamma-\alpha}{\alpha}}$;
(iii) $\alpha\mu - \gamma - 1 < \frac{-\alpha}{r}e^{\frac{1+\gamma-\alpha}{\alpha}}$.

Proof: Upon solving the characteristic equation (3) of the Jacobian matrix J for the linearized system of the model (1) at the equilibrium point E_2, the following results are obtained:

$$p(x,y) = \frac{((\mu+1)\alpha - 1 - \gamma)r(1+\gamma)e^{\frac{\alpha-1-\gamma}{\alpha}} + 2\alpha^2}{\alpha^2},$$

$$q(x,y) = \frac{-r(1+\gamma)\left(\alpha^2\mu + (-\mu-\gamma-2)\alpha + 1 + \gamma\right) e^{\frac{\alpha-1-\gamma}{\alpha}}}{\alpha^2} - \gamma,$$

the local asymptotic stability of the positive equilibrium point E_2 is achieved if the following conditions are met:

$$|p(x,y)| < 1 + q(x,y) < 2,$$

the criterion $1 + p(x,y) + q(x,y) > 0$ can be observed to be equivalent to the condition

$$\alpha^2\mu - (2\mu+\gamma+3)\alpha + 2\alpha + 2 < \frac{\alpha^2(3-\gamma)}{\gamma+1} e^{\frac{1+\gamma-\alpha}{\alpha}},$$

we can easily observe that the criterion $1 - q(x,y) > 0$ is equivalent to

$$\alpha^2\mu - (\mu+\gamma+2)\alpha + \gamma + 1 < \frac{-\alpha^2}{r} e^{\frac{1+\gamma-\alpha}{\alpha}},$$

the condition expressed by the criterion $1-p(x,y)+q(x,y) > 0$ can be rephrased as follows:

$$\alpha\mu - \gamma - 1 < \frac{-\alpha}{r} e^{\frac{1+\gamma-\alpha}{\alpha}}.$$

□

The stability analysis of a nonhyperbolic fixed point can be more complex. When one of the eigenvalues is on the unit circle and the other is inside the unit circle, there are various possibilities to consider. In such cases, centre manifold theory is often used to determine the stability of the fixed point [2, 23, 24].

Lemma 3.1. The stability of E_2 is lost in one of the following two cases:

(i) via a flip point when $(\mu+1)\alpha - \gamma - 1 < \frac{-2\alpha^2}{r(\gamma+1)} e^{\frac{\gamma+1-\alpha}{\alpha}}$, and $\alpha^2\mu - (2\mu+\gamma+3)\alpha + 2\alpha + 2 = \frac{\alpha^2(3-\gamma)}{\gamma+1} e^{\frac{1+\gamma-\alpha}{\alpha}}$;

(ii) via a Neimark-Sacker point when $|((\mu+1)\alpha - \gamma - 1)(\gamma+1) r e^{\frac{\alpha-\gamma-1}{\alpha}} + 2\alpha^2| < -\left(\alpha^2\mu + (-\mu-\gamma-2)\alpha + \gamma + 1\right)(\gamma+1) r e^{\frac{\alpha-\gamma-1}{\alpha}} - \alpha^2(\gamma-1)$, and $\alpha^2\mu - (\mu+\gamma+2)\alpha + \gamma + 1 = \frac{-\alpha^2}{r} e^{\frac{1+\gamma-\alpha}{\alpha}}$; □

4. Bifurcations Analysis

4.1. Neimark-Sacker Bifurcation About E_2

First, we will discuss the Neimark-Sacker bifurcation of the discrete-time model (1) around the equilibrium point E_2. Let us consider the parameter r in a small neighborhood of r^*, i.e., $r = r^* + \epsilon$, where $\epsilon \ll 1$. Then, the discrete-time model (1) can be written as:

$$x_{n+1} = x_n\Big((r^*+\epsilon) e^{(1-x_n)}(x_n-\mu) - \delta y_n\Big), y_{n+1} = y_n(\alpha x_n - \gamma). \quad (5)$$

The characteristic equation of the Jacobian matrix $J\Big(E_2(\frac{\gamma+1}{\alpha}, -\frac{(r^*+\epsilon)(\alpha\mu-\gamma-1)e^{\frac{\alpha-\gamma-1}{\alpha}}+\alpha}{\delta\alpha})\Big)$ of the model (5) about $E_2(\frac{\gamma+1}{\alpha}, -\frac{(r^*+\epsilon)(\alpha\mu-\gamma-1)e^{\frac{\alpha-\gamma-1}{\alpha}}+\alpha}{\delta\alpha})$ is

$$\sigma^2 - p(\epsilon)\sigma + q(\epsilon) = 0,$$

where

$$p(\epsilon) = \frac{(\gamma+1)((\mu+1)\alpha-\gamma-1)(r+\epsilon)e^{\frac{\alpha-\gamma-1}{\alpha}} + 2\alpha^2}{\alpha^2},$$

and

$$q(\epsilon) = -\frac{(\gamma+1)(r+\epsilon)\left(\alpha^2\mu + (-\mu-\gamma-2)\alpha + \gamma + 1\right) e^{\frac{\alpha-\gamma-1}{\alpha}} + \alpha^2\gamma}{\alpha^2}.$$

The solutions to the characteristic equation of $J(E_2)$ are

$$\sigma_{1,2} = \frac{p(\epsilon) \pm \iota\sqrt{4q(\epsilon) - p^2(\epsilon)}}{2},$$

$$= \frac{(\gamma+1)((\mu+1)\alpha-\gamma-1)(r+\epsilon)e^{\frac{\alpha-\gamma-1}{\alpha}} + 2\alpha^2}{2\alpha^2} \pm \frac{\iota}{2}\sqrt{-\frac{(\gamma+1)\left((\gamma+1)((\mu+1)\alpha-\gamma-1)^2(r+\epsilon)^2\left(e^{\frac{\alpha-\gamma-1}{\alpha}}\right)^2 + 4\alpha^3(r+\epsilon)(\mu\alpha-\gamma-1)e^{\frac{\alpha-\gamma-1}{\alpha}} + 4\alpha^4\right)}{\alpha^4}},$$

$$|\sigma_{1,2}| = \sqrt{q(\epsilon)} = \sqrt{-\frac{(\gamma+1)(r+\epsilon)(\alpha^2\mu + (-\mu-\gamma-2)\alpha + \gamma + 1)e^{\frac{\alpha-\gamma-1}{\alpha}} + \alpha^2\gamma}{\alpha^2}},$$

and

$$\left.\frac{d\,|\sigma_{1,2}|}{d\epsilon}\right|_{\epsilon=0} = -\frac{(\gamma+1)e^{\frac{\alpha-\gamma-1}{\alpha}}\left(\alpha^2\mu - (\mu+\gamma+2)\alpha + \gamma + 1\right)}{2\alpha\sqrt{-r(\gamma+1)\left(\alpha^2\mu + (-\mu-\gamma-2)\alpha + \gamma + 1\right)e^{\frac{\alpha-\gamma-1}{\alpha}} - \alpha^2\gamma}} > 0.$$

Furthermore, we imposed the condition that when $\epsilon = 0$, the eigenvalues $\sigma_{1,2}^m$ should not be equal to 1 for $m = 1, 2, 3, 4$. This is equivalent to the condition $p(0) \neq -2, 0, 1, 2$, which can be verified through computation.

The equilibrium E_2 of the discrete-time model (1) is transformed into $O(0, 0)$ when we let $u_n = x_n - x^*$ and $v_n = y_n - y^*$. After some manipulation, we obtain:

$$\begin{aligned} u_{n+1} &= (u_n + x^*)\Big((r^* + \epsilon)\left(u_n + x^* - \mu\right)\mathrm{e}^{(1-u_n-x^*)} - \delta(v_n + y^*)\Big) - x^*, \\ v_{n+1} &= (v_n + y^*)\left(\alpha(u_n + x^*) - \gamma\right) - y^*. \end{aligned} \tag{6}$$

where $x^* = \frac{\gamma+1}{\alpha}, y^* = -\frac{r(\alpha\mu-\gamma-1)\mathrm{e}^{\frac{\alpha-\gamma-1}{\alpha}}+\alpha}{\delta\alpha}$. In the following analysis, we consider the case where $\epsilon = 0$, and we study the normal form of System (6). To obtain the normal form, we expand (6) up to third order using a Taylor series centered at $(u_n, v_n) = (0, 0)$, yielding:

$$\begin{aligned} u_{n+1} &= \Delta_{11}u_n + \Delta_{12}v_n + \Delta_{13}u_n^2 + \Delta_{14}u_n v_n + \Delta_{15}u_n^3 + O(|u_n|, |v_n|)^4, \\ v_{n+1} &= \Delta_{21}u_n + \Delta_{22}v_n + \Delta_{23}u_n v_n, \end{aligned}$$

where

$$\begin{aligned} \Delta_{11} &= r^*\big(-(x^*)^2 + (\mu+2)x^* - \mu\big)\mathrm{e}^{1-x^*} - \delta y^*, \\ \Delta_{12} &= -\delta x^*, \\ \Delta_{13} &= -\frac{r^* y^* \Big(-(x^*)^2 + (\mu+4)x^* - 2\mu - 2\Big)\mathrm{e}^{1-x^*}}{2}, \\ \Delta_{14} &= -\delta, \quad \Delta_{15} = \frac{r^* \Big(-(x^*)^2 + (\mu+6)x^* - 3\mu - 6\Big)\mathrm{e}^{1-x^*}}{6}, \\ \Delta_{21} &= \alpha y^*, \quad \Delta_{22} = \alpha x^* - \gamma, \quad \Delta_{23} = \alpha, \end{aligned}$$

Now, let

$$\begin{aligned} \eta &= \frac{(\gamma+1)((\mu+1)\alpha-\gamma-1)(r+\epsilon)\mathrm{e}^{\frac{\alpha-\gamma-1}{\alpha}} + 2\alpha^2}{2\alpha^2}, \\ \zeta &= \frac{1}{2}\sqrt{-\frac{(\gamma+1)\left((\gamma+1)((\mu+1)\alpha-\gamma-1)^2(r+\epsilon)^2\left(e^{\frac{\alpha-\gamma-1}{\alpha}}\right)^2 + 4\alpha^3(r+\epsilon)(\mu\alpha-\gamma-1)e^{\frac{\alpha-\gamma-1}{\alpha}} + 4\alpha^4\right)}{\alpha^4}}, \end{aligned}$$

The matrix T, which is invertible, is defined by

$$T = \begin{pmatrix} \Delta_{12} & 0 \\ \eta - \Delta_{11} & -\zeta \end{pmatrix}.$$

By employing the subsequent transformation:

$$\begin{pmatrix} u_n \\ v_n \end{pmatrix} = \begin{pmatrix} \Delta_{12} & 0 \\ \eta - \Delta_{11} & -\zeta \end{pmatrix} \begin{pmatrix} X_n \\ Y_n \end{pmatrix},$$

(6) gives

$$\begin{pmatrix} X_{n+1} \\ Y_{n+1} \end{pmatrix} = \begin{pmatrix} \eta & -\zeta \\ \zeta & \eta \end{pmatrix} \begin{pmatrix} X_n \\ Y_n \end{pmatrix} + \begin{pmatrix} \Gamma(X_n, Y_n) \\ \Pi(X_n, Y_n) \end{pmatrix}, \tag{7}$$

where

$$\begin{aligned} \Gamma(X_n, Y_n) &= \Lambda_{11}{X_n}^2 + \Lambda_{12}X_nY_n + \Lambda_{13}X_n^3, \\ \Pi(X_n, Y_n) &= \Lambda_{21}{X_n}^2 + \Lambda_{22}X_nY_n + \Lambda_{23}X_n^3, \end{aligned}$$

and

$$\begin{aligned} \Lambda_{11} &= \Delta_{14}(\eta - \Delta_{11}) + \Delta_{12}\Delta_{13}, \\ \Lambda_{12} &= -\zeta\Delta_{14}, \\ \Lambda_{13} &= \Delta_{12}^2\Delta_{15}, \\ \Lambda_{21} &= \frac{1}{\zeta}(\eta - \Delta_{11})\Big(\eta\Delta_{14} - \Delta_{14}\Delta_{11} + (\Delta_{13} - \Delta_{24})\Delta_{12}\Big), \\ \Lambda_{22} &= \Delta_{14}(\Delta_{11} - \eta) + \Delta_{24}\Delta_{12}, \\ \Lambda_{23} &= \frac{1}{\zeta}(\eta - \Delta_{11})\Delta_{15}\Delta_{12}^2. \end{aligned}$$

In addition,

$$\begin{aligned}
&\Gamma_{X_nX_n}|_{(0,0)} = 2\Lambda_{11},\ \Gamma_{X_nY_n}|_{(0,0)} = \Lambda_{12},\ \Gamma_{Y_nY_n}|_{(0,0)} = 0,\\
&\Gamma_{X_nX_nX_n}|_{(0,0)} = 6\Lambda_{13},\ \Gamma_{X_nX_nY_n}|_{(0,0)} = 0,\\
&\Gamma_{X_nY_nY_n}|_{(0,0)} = \Gamma_{Y_nY_nY_n}|_{(0,0)} = 0,
\end{aligned}$$

and

$$\begin{aligned}
&\Pi_{X_nX_n}|_{(0,0)} = 2\Lambda_{21},\ \Pi_{X_nY_n}|_{(0,0)} = \Lambda_{22},\ \Pi_{Y_nY_n}|_{(0,0)} = 0,\\
&\Pi_{X_nX_nX_n}|_{(0,0)} = 6\Lambda_{23}.\ \Pi_{X_nX_nY_n}|_{(0,0)} = 0\\
&\Pi_{X_nY_nY_n}|_{(0,0)} = \Pi_{Y_nY_nY_n}|_{(0,0)} = 0.
\end{aligned}$$

For a Neimark-Sacker bifurcation to occur in (7), it is necessary that the discriminant χ is non-zero (see [2, 23, 25])

$$\chi = -\operatorname{Re}\left[\frac{(1-2\bar{\sigma})\bar{\sigma}^2}{1-\sigma}\theta_{11}\theta_{20}\right] - \frac{1}{2}\|\theta_{11}\|^2 - \|\theta_{02}\|^2 + \operatorname{Re}(\bar{\sigma}\theta_{21}),$$

where

$$\begin{aligned}
\theta_{02} &= \frac{1}{8}\big[\Gamma_{X_nX_n} - \Gamma_{Y_nY_n} + 2\Pi_{X_nY_n} + \iota\big(\Pi_{X_nX_n} - \Pi_{Y_nY_n} + 2\Gamma_{X_nY_n}\big)\big]\Big|_{(0,0)},\\
\theta_{11} &= \frac{1}{4}\left[\Gamma_{X_nX_n} + \Gamma_{Y_nY_n} + \iota\left(\Pi_{X_nX_n} + \Pi_{Y_nY_n}\right)\right]\Big|_{(0,0)},\\
\theta_{20} &= \frac{1}{8}\big[\Gamma_{X_nX_n} - \Gamma_{Y_nY_n} + 2\Pi_{X_nY_n} + \iota\big(\Pi_{X_nX_n} - \Pi_{Y_nY_n} - 2\Gamma_{X_nY_n}\big)\big]\Big|_{(0,0)},\\
\theta_{21} &= \frac{1}{16}\big[\Gamma_{X_nX_nX_n} + \Gamma_{X_nY_nY_n} + \Pi_{X_nX_nY_n} + \Pi_{Y_nY_nY_n}\\
&\quad + \iota\left(\Pi_{X_nX_nX_n} + \Pi_{X_nY_nY_n} - \Gamma_{X_nX_nY_n} - \Gamma_{Y_nY_nY_n}\right)\big]\Big|_{(0,0)}.
\end{aligned}$$

Upon computation, the result is obtained as follows:

$$\begin{aligned}
\theta_{02} &= \tfrac{1}{4}\left[\Lambda_{11} + \Lambda_{22} + \iota\left(\Lambda_{21} + \Lambda_{12}\right)\right],\\
\theta_{11} &= \tfrac{1}{2}\left[\Lambda_{11} + \iota\Lambda_{21}\right],\\
\theta_{20} &= \tfrac{1}{4}\left[\Lambda_{11} + \Lambda_{22} + \iota\left(\Lambda_{21} - \Lambda_{12}\right)\right],\\
\theta_{21} &= \tfrac{3}{8}\left[\Lambda_{13} + \iota\Lambda_{23}\right].
\end{aligned}$$

After analyzing the normal form and using the Neimark-Sacker bifurcation theorem discussed in various sources including [23, 26–29], we can conclude the following proposition.

Proposition 4.1. Provided that the parameters satisfy condition (2) in Lemma (3.1), a Neimark-Sacker bifurcation occurs about E_2 in the discrete-time model (1) when $\chi \neq 0$. Moreover, if $\chi < 0$ (resp. $\chi > 0$), an attracting (resp. repelling) closed curve emerges from E_2.

Remark 4.1. A supercritical Neimark-Sacker bifurcation occurs in the discrete-time model (1) if the discriminatory quantity $\chi < 0$ according to bifurcation theory discussed in [27].

4.2. Period-doubling Bifurcation

This section focuses on investigating the period-doubling bifurcation of model (1) at E_2 in a small neighborhood of condition (i) from Lemma (3.1) by selecting arbitrary parameters $(\alpha, r, \delta, \gamma, \mu)$. Here, we treating r^* as a new dependent variable. As a result, we obtain:

$$\begin{aligned}
x_{n+1} &= x_n\Big(\left(r + r^*\right)\mathrm{e}^{(1-x_n)}\big(x_n - \mu\big) - \delta y_n\Big),\\
y_{n+1} &= y_n\left(\alpha x_n - \gamma\right).
\end{aligned} \tag{8}$$

Let $u_n = x_n - x^*$ and $v_n = y_n - y^*$. The equilibrium E_2 of model (8) is transformed into $O(0,0)$ by this coordinate transformation. We expand the model (8) as a Taylor series up to the third order around $(u_n, u_n, r^*) = (0,0,0)$, which results in the following model.

$$\begin{aligned}
u_{n+1} &= \widehat{\Delta_{11}}u_n + \widehat{\Delta_{12}}v_n + \widehat{\Delta_{13}}u_n^2 + \widehat{\Delta_{14}}u_nv_n + \widehat{\Delta_{15}}u_nr^* + \widehat{\Delta_{16}}u_n^3 + \widehat{\Delta_{17}}u_n^2r^* + O\left(|u_n|, |r^*|\right)^4,\\
v_{n+1} &= \widehat{\Delta_{21}}u_n + \widehat{\Delta_{22}}v_n + \widehat{\Delta_{23}}u_nv_n,
\end{aligned} \tag{9}$$

where

$$\begin{aligned}
\widehat{\Delta_{11}} &= r\big(-(x^*)^2+(\mu+2)x^*-\mu\big)\mathrm{e}^{1-x^*}-\delta y^*,\\
\widehat{\Delta_{12}} &= -\delta x^*,\\
\widehat{\Delta_{13}} &= -\frac{r}{2}\big(-(x^*)^2+(\mu+4)x^*-2\mu-2\big)\mathrm{e}^{1-x^*},\\
\widehat{\Delta_{14}} &= -\delta,\\
\widehat{\Delta_{15}} &= \big(-(x^*)^2+(\mu+2)x^*-\mu\big)\mathrm{e}^{1-x^*},\\
\widehat{\Delta_{16}} &= \frac{r}{6}\big(-(x^*)^2+(\mu+6)x^*-3\mu-6\big)\mathrm{e}^{1-x^*},\\
\widehat{\Delta_{17}} &= -\frac{1}{2}\big(-(x^*)^2+(\mu+4)x^*-2\mu-2\big)\mathrm{e}^{1-x^*},\\
\widehat{\Delta_{21}} &= \alpha y^*,\quad \widehat{\Delta_{22}}=\alpha x^*-\gamma,\quad \widehat{\Delta_{23}}=\alpha.
\end{aligned}$$

Construct an invertible matrix T as follows

$$T=\begin{pmatrix}\widehat{\Delta_{12}} & \widehat{\Delta_{12}}\\ -1-\widehat{\Delta_{11}} & \sigma_2-\widehat{\Delta_{11}}\end{pmatrix},$$

and use the translation

$$\begin{pmatrix}u_n\\ v_n\end{pmatrix}=\begin{pmatrix}\widehat{\Delta_{12}} & \widehat{\Delta_{12}}\\ -1-\widehat{\Delta_{11}} & \sigma_2-\widehat{\Delta_{11}}\end{pmatrix}\begin{pmatrix}X_n\\ Y_n\end{pmatrix},$$

(9) gives

$$\begin{pmatrix}X_{n+1}\\ Y_{n+1}\end{pmatrix}=\begin{pmatrix}-1 & 0\\ 0 & \sigma_2\end{pmatrix}\begin{pmatrix}X_n\\ Y_n\end{pmatrix}+\begin{pmatrix}\widehat{\Gamma}(u_n,v_n,r^*)\\ \widehat{\Pi}(u_n,v_n,r^*)\end{pmatrix}, \tag{10}$$

where

$$\begin{aligned}
\widehat{\Gamma}(u_n,v_n,r^*) =& \frac{\widehat{\Delta_{13}}\left(\sigma_2-\widehat{\Delta_{11}}\right)}{\widehat{\Delta_{12}}(1+\sigma_2)}u_n^2+\frac{\widehat{\Delta_{15}}\left(\sigma_2-\widehat{\Delta_{11}}\right)}{\widehat{\Delta_{12}}(1+\sigma_2)}u_nr^*+\frac{\widehat{\Delta_{14}}\left(\sigma_2-\widehat{\Delta_{11}}\right)-\widehat{\Delta_{23}}\widehat{\Delta_{12}}}{\widehat{\Delta_{12}}(1+\sigma_2)}u_nv_n\\
+& \frac{\widehat{\Delta_{17}}\left(\sigma_2-\widehat{\Delta_{11}}\right)}{\widehat{\Delta_{12}}(1+\sigma_2)}u_n^2r^*+\frac{\widehat{\Delta_{16}}\left(\sigma_2-\widehat{\Delta_{11}}\right)}{\widehat{\Delta_{12}}(1+\sigma_2)}u_n^3+O\left(|u_n|,|r^*|\right)^4,\\
\widehat{\Pi}(u_n,v_n,r^*) =& \frac{\widehat{\Delta_{13}}\left(1+\widehat{\Delta_{11}}\right)}{\widehat{\Delta_{12}}(1+\sigma_2)}u_n^2+\frac{\widehat{\Delta_{15}}\left(1+\widehat{\Delta_{11}}\right)}{\widehat{\Delta_{12}}(1+\sigma_2)}u_nr^*+\frac{\widehat{\Delta_{14}}\left(1+\widehat{\Delta_{11}}\right)+\widehat{\Delta_{12}}\widehat{\Delta_{23}}}{\widehat{\Delta_{12}}(1+\sigma_2)}u_nv_n\\
+& \frac{\widehat{\Delta_{17}}\left(1+\widehat{\Delta_{11}}\right)}{\widehat{\Delta_{12}}(1+\sigma_2)}u_n^2r^*+\frac{\widehat{\Delta_{16}}\left(1+\widehat{\Delta_{11}}\right)}{\widehat{\Delta_{12}}(1+\sigma_2)}u_n^3+O\left(|u_n|,|r^*|\right)^4.
\end{aligned}$$

$$\begin{aligned}
u_n^2 =& \widehat{\Delta_{12}}^2\left(X_n^2+2X_nY_n+Y_n^2\right),\\
u_nv_n =& -\widehat{\Delta_{12}}\left(1+\widehat{\Delta_{11}}\right)X_n^2+\left(\widehat{\Delta_{12}}(\sigma_2-\widehat{\Delta_{11}})-\widehat{\Delta_{12}}\left(1+\widehat{\Delta_{11}}\right)\right)X_nY_n+\widehat{\Delta_{12}}\left(\sigma_2-\widehat{\Delta_{11}}\right)Y_n^2,\\
u_nr^* =& \widehat{\Delta_{12}}X_nr^*+\widehat{\Delta_{12}}Y_nr^*,\\
u_n^2r^* =& \widehat{\Delta_{12}}^2\left(X_n^2r^*+2X_nY_nr^*+Y_n^2r^*\right).
\end{aligned}$$

According to the center manifold theorem [23, 27, 30, 31], we can construct a center manifold $W^c(0,0)$ of (10) about $(0,0)$ in a small neighborhood of r^*. The center manifold can be represented as follows:

$$W^c(0,0)=\left\{(X_n,Y_n): Y_n=c_0r^*+c_1X_n^2+c_2X_nr^*+c_3(r^*)^2+O\left((|X_n|,|r^*|)^3\right)\right\},$$

The function $O\left((|X_n|+|r|)^3\right)$ is order three or higher in the variables (X_n,r), representing the higher-order terms that are neglected in the expansion, and

$$c_0 = 0,\ c_1 = \frac{\left(1+\widehat{\Delta_{11}}\right)\left(\widehat{\Delta_{11}}\widehat{\Delta_{14}} + (\widehat{\Delta_{23}} - \widehat{\Delta_{13}})\widehat{\Delta_{12}} + \widehat{\Delta_{14}}\right)}{\sigma_2^2 - 1},$$

$$c_2 = -\frac{\widehat{\Delta_{15}}\left(1+\widehat{\Delta_{11}}\right)}{(1+\sigma_2)^2},\ c_3 = 0.$$

Thus, we can restrict the map (10) to the center manifold $W^c(0,0)$ and obtain the following map:

$$f\left(X_n\right) = -X_n + h_1 X_n^2 + h_2 X_n r^* + h_3 X_n^2 r^* + h_4 X_n (r^*)^2 + h_5 X_n^3 + O\left(\left(\left|X_n\right|, \left|r^*\right|\right)^4\right), \tag{11}$$

where

$$\begin{aligned}
h_1 =& \frac{1}{1+\sigma_2}\left[\widehat{\Delta_{11}}^2\widehat{\Delta_{14}} + \left(\left(\widehat{\Delta_{23}} - \widehat{\Delta_{13}}\right)\widehat{\Delta_{12}} - \widehat{\Delta_{14}}\left(\sigma_2 - 1\right)\right)\widehat{\Delta_{11}} + \left(\sigma_2\widehat{\Delta_{13}} + \widehat{\Delta_{23}}\right)\widehat{\Delta_{12}} - \sigma_2\widehat{\Delta_{14}}\right],\\
h_2 =& \frac{1}{1+\sigma_2}\left[\widehat{\Delta_{15}}\left(\sigma_2 - \widehat{\Delta_{11}}\right)\right],\\
h_3 =& \frac{1}{(\sigma_2-1)(\sigma_2+1)^3}\Big[\sigma_2^4\widehat{\Delta_{12}}\widehat{\Delta_{17}} - \big(\widehat{\Delta_{14}}(\widehat{\Delta_{11}}+1)\widehat{\Delta_{15}} + \widehat{\Delta_{12}}\widehat{\Delta_{17}}(\widehat{\Delta_{11}}-1)\big)\sigma_2^3\\
&+ 4\Big(((-\frac{3}{4}\widehat{\Delta_{13}} + \frac{1}{2}\widehat{\Delta_{23}})\widehat{\Delta_{12}} + \widehat{\Delta_{14}}(\widehat{\Delta_{11}} + \frac{3}{4}))\widehat{\Delta_{15}} - \frac{1}{4}\widehat{\Delta_{17}}\widehat{\Delta_{12}}\Big)(\widehat{\Delta_{11}}+1)\sigma_2^2\\
&+ \Big(-3\big(-(\widehat{\Delta_{13}} - \widehat{\Delta_{23}})(\widehat{\Delta_{11}} + \frac{1}{3})\widehat{\Delta_{12}} + \widehat{\Delta_{11}}\widehat{\Delta_{14}}(\widehat{\Delta_{11}} + \frac{3}{4})\big)(\widehat{\Delta_{11}}+1)\widehat{\Delta_{15}}\\
&+ \widehat{\Delta_{12}}\widehat{\Delta_{17}}(\widehat{\Delta_{11}}-1)\Big)\sigma_2 + \Big(((\widehat{\Delta_{23}} - \widehat{\Delta_{13}})\widehat{\Delta_{11}} + \widehat{\Delta_{23}})\widehat{\Delta_{12}} + \widehat{\Delta_{11}}^2\widehat{\Delta_{14}}\Big)(\widehat{\Delta_{11}}+1)\widehat{\Delta_{15}} + \widehat{\Delta_{11}}\widehat{\Delta_{12}}\widehat{\Delta_{17}}\Big],\\
h_4 =& \frac{\widehat{\Delta_{11}}^2\left(\sigma_2 - \widehat{\Delta_{11}}\right)\left(1+\widehat{\Delta_{11}}\right)}{\left(\sigma_2+1\right)^3},
\end{aligned}$$

$$\begin{aligned}
h_5 =& \frac{1}{(\sigma_2-1)(\sigma_2+1)^2}\Big[\Big(2(\widehat{\Delta_{13}} - \widehat{\Delta_{23}})^2\widehat{\Delta_{11}}^2 + \big(-\sigma_2^2\widehat{\Delta_{16}} + (3\widehat{\Delta_{23}}\widehat{\Delta_{13}} - 2\widehat{\Delta_{13}}^2 - \widehat{\Delta_{23}}^2)\sigma_2\\
&+ 2\widehat{\Delta_{13}}^2 - 5\widehat{\Delta_{23}}\widehat{\Delta_{13}} + 3\widehat{\Delta_{23}}^2 + \widehat{\Delta_{16}}\big)\widehat{\Delta_{11}} + \sigma_2^3\widehat{\Delta_{16}} + (3\widehat{\Delta_{23}}\widehat{\Delta_{13}} - 2\widehat{\Delta_{13}}^2\\
&- \widehat{\Delta_{23}}^2 - \widehat{\Delta_{16}})\sigma_2 - \widehat{\Delta_{23}}(\widehat{\Delta_{13}} - \widehat{\Delta_{23}})\Big)\widehat{\Delta_{12}}^2 - \widehat{\Delta_{14}}(\widehat{\Delta_{11}}+1)\Big(4(\widehat{\Delta_{13}}\\
&- \widehat{\Delta_{23}})\widehat{\Delta_{11}}^2 + \big((4\widehat{\Delta_{23}} - 5\widehat{\Delta_{13}})\sigma_2 + 3\widehat{\Delta_{13}} - 4\widehat{\Delta_{23}}\big)\widehat{\Delta_{11}} + (\widehat{\Delta_{13}} - \widehat{\Delta_{23}})\sigma_2^2 + (2\widehat{\Delta_{23}} - 3\widehat{\Delta_{13}})\sigma_2 - \widehat{\Delta_{23}}\Big)\widehat{\Delta_{12}}\\
&+ \widehat{\Delta_{14}}^2(\widehat{\Delta_{11}}+1)^2(\sigma_2 - \widehat{\Delta_{11}})(\sigma_2 - 2\widehat{\Delta_{11}} - 1)\Big].
\end{aligned}$$

For a period-doubling bifurcation to occur in the map (11), it is necessary that the following discriminatory quantities are nonzero:

$$\Delta_1 = \left(\frac{\partial^2 f}{\partial X_n \partial r^*} + \frac{1}{2}\frac{\partial f}{\partial r^*}\frac{\partial^2 f}{\partial X_n^2}\right)\Bigg|_{(0,0)},\ \Delta_2 = \left(\frac{1}{6}\frac{\partial^3 f}{\partial X_n^3} + \left(\frac{1}{2}\frac{\partial^2 f}{\partial X_n^2}\right)^2\right)\Bigg|_{(0,0)}.$$

After calculating we obtain

$$\Delta_1 = h_2 + \frac{1}{2}h_3,$$

and

$$\Delta_2 = h_5 + h_1^2.$$

Based on the analysis in [22] and the bifurcation theory in [23, 26–29], we can propose the following proposition.

Proposition 4.2. Assuming that $\Delta_2 \neq 0$, the discrete-time model (8) exhibits a period-doubling bifurcation at the unique positive equilibrium E_2, when r^* varies within a small neighborhood of $O(0,0)$. Furthermore, the stability of the period-2 points emerging from E_2 depends on the sign of Δ_2; the bifurcated points are stable if $\Delta_2 > 0$, and unstable if $\Delta_2 < 0$.

5. Numerical Simulations

This section presents numerical simulations to demonstrate the complex dynamical behavior of model (1). Bifurcation diagrams and phase portraits are utilized as visual aids to provide further evidence of the theoretical analysis discussed earlier.

We start by selecting the parameter values as $\delta = 0.1$, $\alpha = 2$, and $\gamma = 5.1$, with an initial condition of $(3.05, 4.75)$. Initially, we construct the bifurcation diagram of the model (1) without considering the Allee effect (Figure (1)-a). As the system evolves, it reaches a stable equilibrium, and subsequently, chaotic dynamics emerge.

To investigate the influence of the Allee effect, we focus on the bifurcation diagram of System (1) with respect to the parameter μ. By gradually increasing the Allee parameter, we observe that the system undergoes a transition. Beyond a critical threshold value of 0.262, the dynamics become stable (Figure (1)-b). This finding is consistent with our theoretical analysis and is further supported by numerical simulations that showcase the novel and intricate dynamical behavior of the model.

Next, we investigate the behavior of model (1) by varying the parameter r within the range $3.8 \le r \le 4.1$. In the interval $3.8 \le r < 4.032$, the model exhibits a unique positive stable equilibrium point. By computation, we find that this equilibrium point is located at $(3.05, 4.793185240)$ for the parameter values $r = 4.032, \delta = 0.1, \mu = 0.2, \alpha = 2, \gamma = 5.1$. The corresponding phase portraits for different values of r within this range are depicted in Figure 3. Notably, at $r = 4.0321$, a Neimark-Sacker bifurcation occurs, as illustrated in Figure 2 (f), with

$$-\frac{(\gamma+1)\mathrm{e}^{\frac{\alpha-\gamma-1}{\alpha}}\left(\alpha^2\mu-(\mu+\gamma+2)\alpha+\gamma+1\right)}{2\alpha\sqrt{-r(\gamma+1)\left(\alpha^2\mu+(-\mu-\gamma-2)\alpha+\gamma+1\right)\mathrm{e}^{\frac{\alpha-\gamma-1}{\alpha}}-\alpha^2\gamma}} = 0.7576542145 > 0$$

hold. Furthermore, for $r = 4.0321$, the eigenvalues of J_{E_2} around E_2 are

$$\sigma_{1,2} = -0.464431894 \pm 0.882896387\iota, \tag{12}$$

After performing calculations, we obtain

$$\begin{aligned}
\theta_{02} &= 0.02191700441 - 0.08872080900\iota,\\
\theta_{11} &= -0.07938575138 - 0.2215864374\iota,\\
\theta_{20} &= 0.01095850221 - 0.06643281419\iota,\\
\theta_{21} &= 0.009076385606 + 0.02533457095\iota,
\end{aligned} \tag{13}$$

Based on the calculations from (12) and (13), the value of the discriminatory quantity is $\chi = -0.08653744470 < 0$. Therefore, when $r = 4.321 > 4.32$, the model (1) undergoes a supercritical Neimark-Sacker bifurcation, resulting in the emergence of a stable invariant closed curve, as shown in Figure 3. As the parameter r exceeds the value of 4.04, chaotic behavior emerges, as observed in Figure 3(b-e).

The numerical solutions depicted in Figure 2 and Figure 3 demonstrate that the stable fixed point E_2 becomes unstable, leading to the coexistence of prey and predator populations through persistent positive periodic oscillations over time.

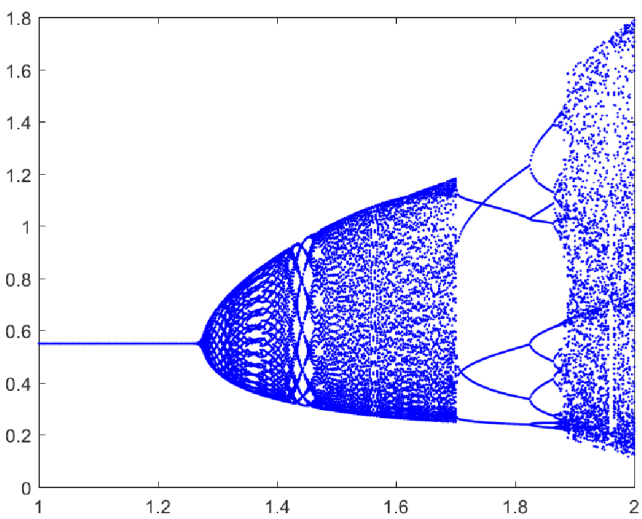

(a) Without Allee effect where the values of parameters are $\delta = 0.1$, $\alpha = 2, \gamma = 0.1$. Corresponding to the bifurcating parameter r.

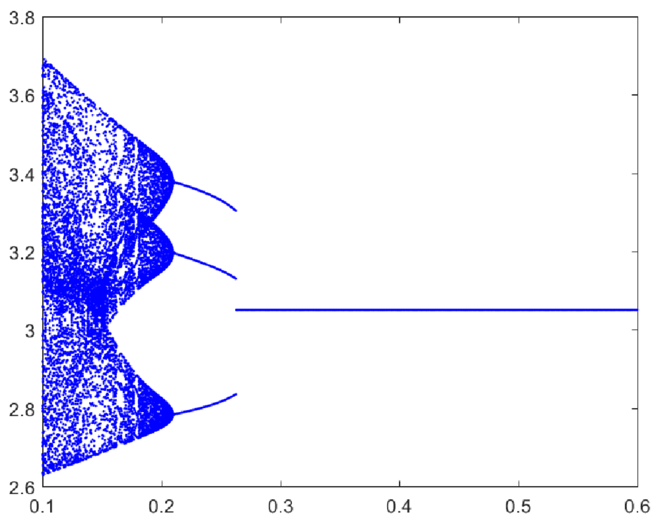

(b) With Allee effect where the values of parameters are $r = 4$, $\delta = 0.1, \alpha = 2, \gamma = 5.1$. Corresponding to the bifurcating parameter μ.

Figure 1. *Bifurcation diagrams.*

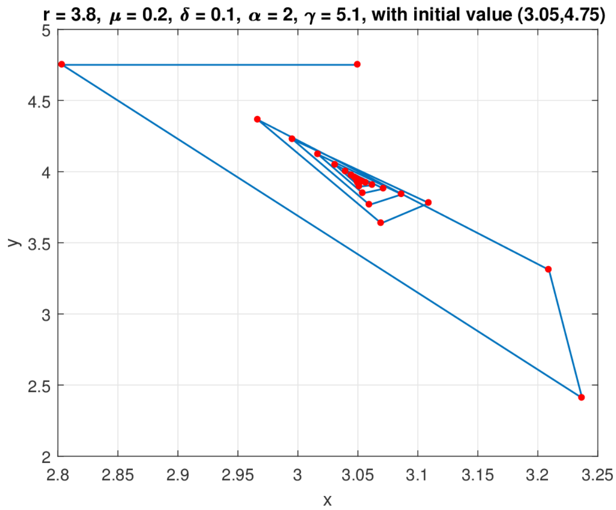

(a) stable equilibrium

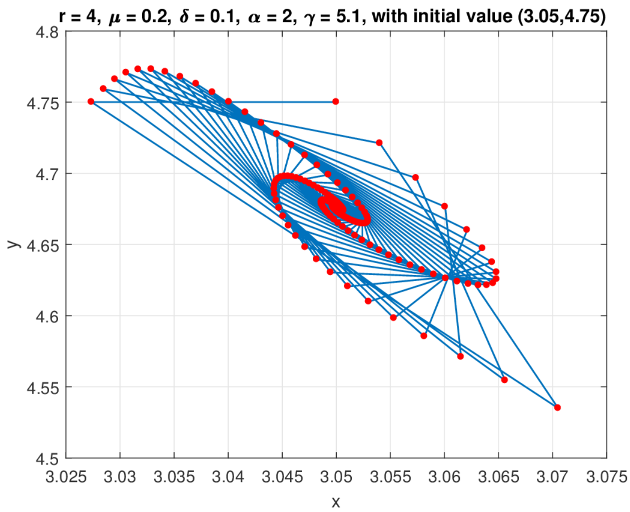

(b) stable equilibrium

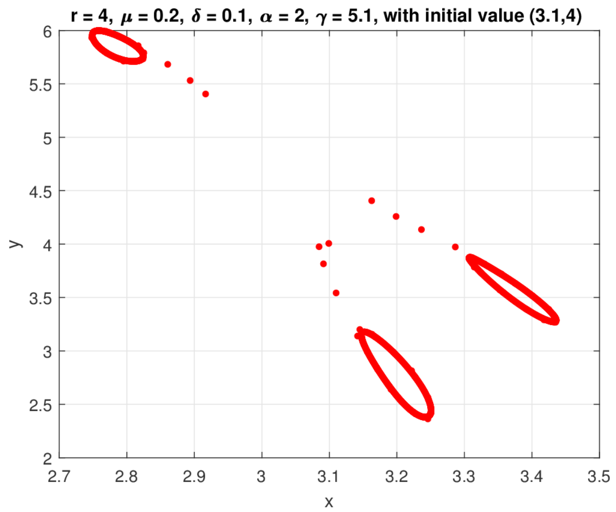

(c) stable equilibrium

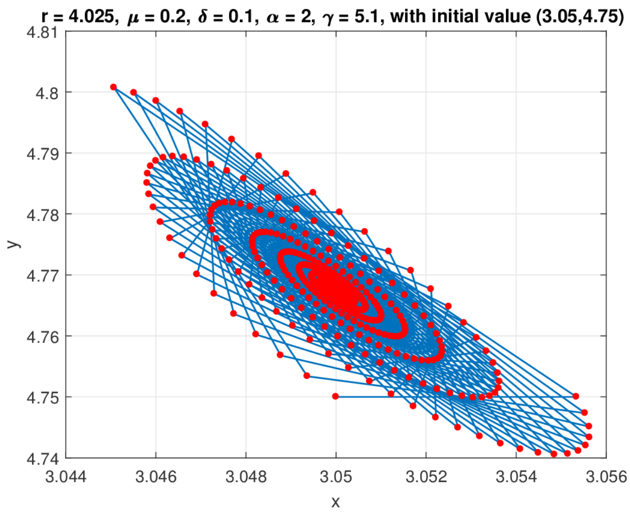

(d) stable equilibrium

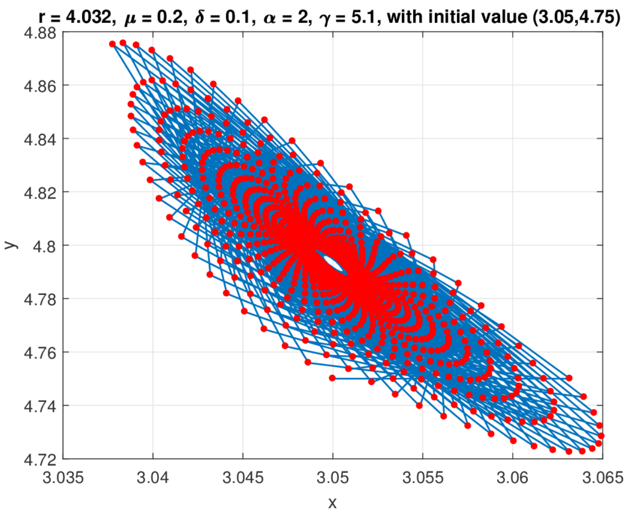

(e) invariant circle

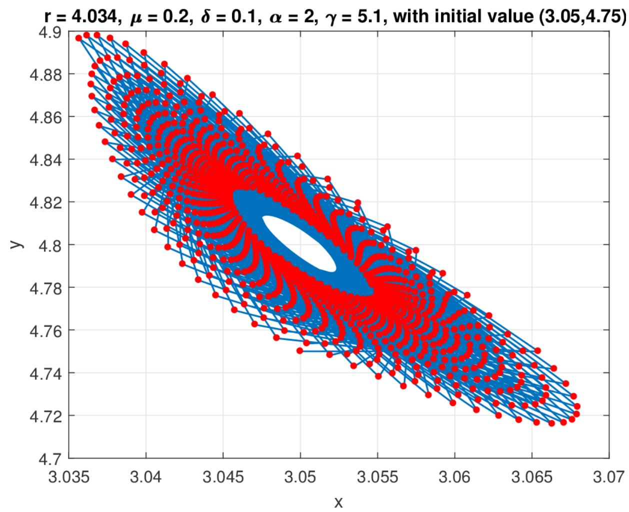

(f) invariant circle

Figure 2. *Phase portraits for various values of r from 3.8 to 4.034.*

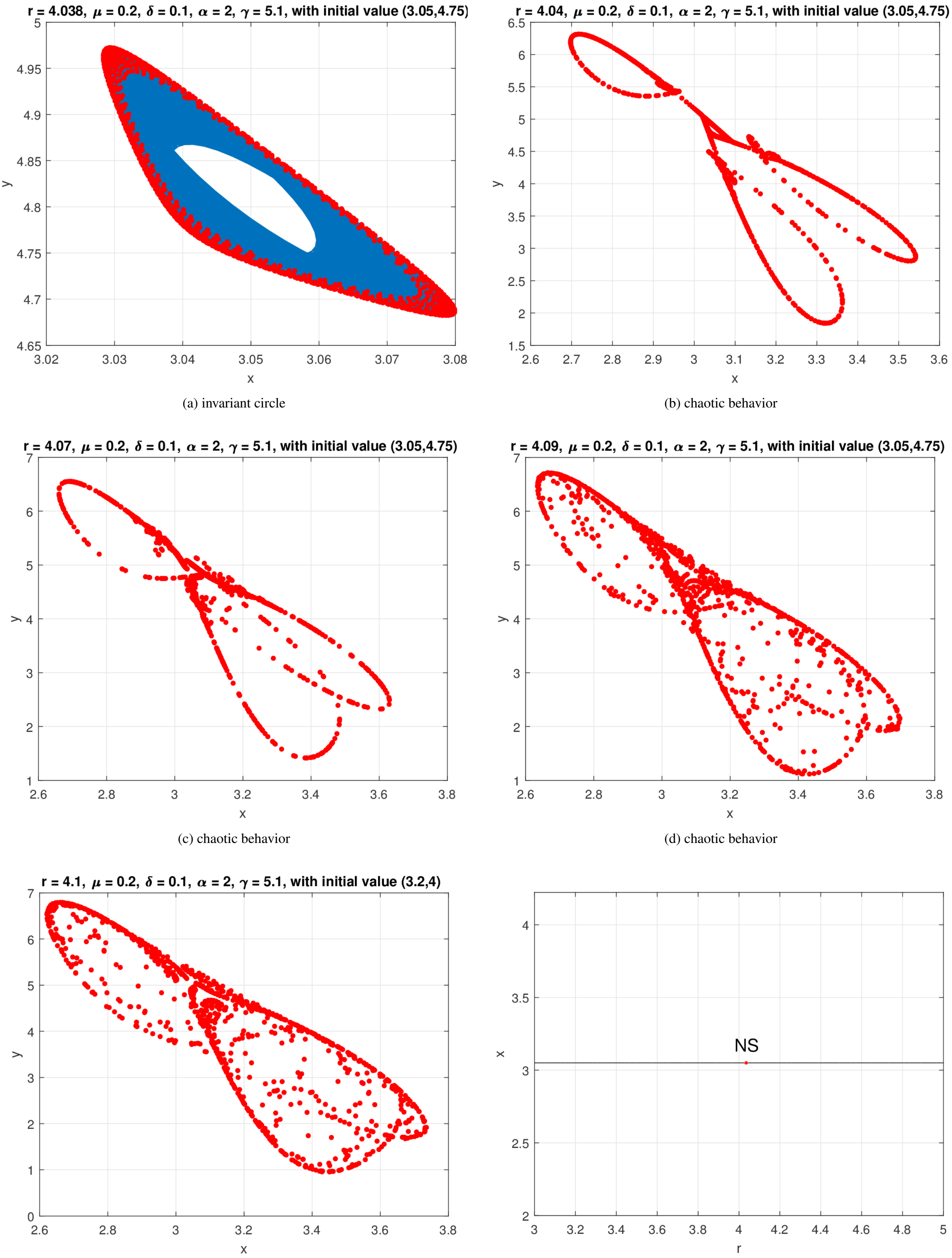

(a) invariant circle

(b) chaotic behavior

(c) chaotic behavior

(d) chaotic behavior

(e) chaotic behavior

(f) Continuation of E_2 in (δ, x)-space.
The branch point (BP), Neimark-Sacker point (NS).

Figure 3. *Phase portraits for various values of r from 4.038 to 4.1.*

6. Conclusions

In conclusion, the stability analysis of predator-prey models with Allee effect is crucial for understanding their biological significance and can inform conservation management. The Allee effect is a natural phenomenon that can have either a stabilizing or destabilizing effect on population dynamics, and its impact on the model can be explored through bifurcation diagram analysis.

In this study, we analyzed a prey-predator model with Allee effect in the prey growth function. By increasing the strength of the Allee parameter, we observed a transition from chaotic behavior to stability in the model dynamics. We also investigated the effect of Allee parameter on the model for different values of μ and produced bifurcation diagrams and phase portraits for various parameter values (Figures (1), (2), and (3)). Our analysis showed that the Allee effect has a stabilizing effect on the model dynamics.

Moreover, by replacing the logistic growth function with the Ricker map, we demonstrated that the behavior of the model dynamics can be altered and enriched. Our results may have significant applications in species conservation management policies. Overall, our study highlights the importance of considering the Allee effect in ecological models and its potential impact on conservation management.

References

[1] J. D. Murray, *Mathematical biology II: Spatial models and biomedical applications*, vol. 3. Springer New York, 2001.

[2] S. N. Elaydi, *Discrete chaos: with applications in science and engineering*. Chapman and Hall/CRC, 2007.

[3] E. S. Allman and J. A. Rhodes, *Mathematical models in biology: an introduction*. Cambridge University Press, 2004.

[4] S. Gao and L. Chen, "The effect of seasonal harvesting on a single-species discrete population model with stage structure and birth pulses," *Chaos, Solitons & Fractals*, vol. 24, no. 4, pp. 1013–1023, 2005.

[5] M. Y. Hamada, T. El-Azab, and H. El-Metwally, "Allee effect in a ricker type predator-prey model," *Journal of Mathematics and Computer Science*, vol. 29, no. 03, pp. 239–251, 2022.

[6] C. Celik and O. Duman, "Allee effect in a discrete-time predator–prey system," *Chaos, Solitons & Fractals*, vol. 40, no. 4, pp. 1956–1962, 2009.

[7] S. Pal, S. K. Sasmal, and N. Pal, "Chaos control in a discrete-time predator–prey model with weak allee effect," *International Journal of Biomathematics*, vol. 11, no. 07, p. 1850089, 2018.

[8] L. Zhang and L. Zou, "Bifurcations and control in a discrete predator–prey model with strong allee effect," *International Journal of Bifurcation and Chaos*, vol. 28, no. 05, p. 1850062, 2018.

[9] A. Morozov, S. Petrovskii, and B.-L. Li, "Bifurcations and chaos in a predator-prey system with the allee effect," *Proceedings of the Royal Society of London. Series B: Biological Sciences*, vol. 271, no. 1546, pp. 1407–1414, 2004.

[10] J. Wang, J. Shi, and J. Wei, "Predator–prey system with strong allee effect in prey," *Journal of Mathematical Biology*, vol. 62, no. 3, pp. 291–331, 2011.

[11] A. J. Terry, "Predator–prey models with component allee effect for predator reproduction," *Journal of mathematical biology*, vol. 71, no. 6, pp. 1325–1352, 2015.

[12] C. Wang and X. Li, "Further investigations into the stability and bifurcation of a discrete predator–prey model," *Journal of Mathematical Analysis and Applications*, vol. 422, no. 2, pp. 920–939, 2015.

[13] M. Y. Hamada, T. El-Azab, and H. El-Metwally, "Bifurcations and dynamics of a discrete predator–prey model of ricker type," *Journal of Applied Mathematics and Computing*, pp. 1–23, 2022.

[14] S. M. Rana *et al.*, "Chaotic dynamics and control of discrete ratio-dependent predator-prey system," *Discrete Dynamics in Nature and Society*, vol. 2017, 2017.

[15] Q. Cui, Q. Zhang, Z. Qiu, and Z. Hu, "Complex dynamics of a discrete-time predator-prey system with holling iv functional response," *Chaos, Solitons & Fractals*, vol. 87, pp. 158–171, 2016.

[16] M. Zhao, C. Li, and J. Wang, "Complex dynamic behaviors of a discrete-time predator-prey system," *Journal of Applied Analysis & Computation*, vol. 7, no. 2, pp. 478–500, 2017.

[17] M. Hamada, T. El-Azab, and H. El-Metwally, "Bifurcations and dynamics of a discrete predator–prey model of ricker type," *Journal of Applied Mathematics and Computing*, vol. 69, no. 1, pp. 113–135, 2023.

[18] A. Q. Khan and H. El-Metwally, "Global dynamics, boundedness, and semicycle analysis of a difference equation," *Discrete Dynamics in Nature and Society*, vol. 2021, 2021.

[19] M. Y. Hamada, T. El-Azab, and H. El-Metwally, "Bifurcation analysis of a two-dimensional discrete-time predator–prey model," *Mathematical Methods in the Applied Sciences*, vol. 46, no. 4, pp. 4815–4833, 2023.

[20] F. Courchamp, L. Berec, and J. Gascoigne, *Allee effects in ecology and conservation*. OUP Oxford, 2008.

[21] Y. Ye, H. Liu, Y.-m. Wei, M. Ma, and K. Zhang, "Dynamic study of a predator-prey model with weak allee effect and delay," *Advances in Mathematical Physics*, vol. 2019, 2019.

[22] H. EL-METWALLY, A. KHAN, and M. HAMADA, "Allee effect in a ricker type discrete-time predator–prey model with holling type-II functional response," *Journal of Biological Systems*, pp. 1–20, 2023.

[23] Y. A. Kuznetsov, *Elements of applied bifurcation theory*, vol. 112. New York: Springer-Verlag, 2004.

[24] S. Wiggins and M. Golubitsky, *Introduction to applied nonlinear dynamical systems and chaos*, vol. 2. Springer, 1990.

[25] X. Liu and D. Xiao, "Complex dynamic behaviors of a discrete-time predator–prey system," *Chaos, Solitons & Fractals*, vol. 32, no. 1, pp. 80–94, 2007.

[26] J. Guckenheimer and P. Holmes, *Nonlinear oscillations, dynamical systems, and bifurcations of vector fields*, vol. 42. Springer Science & Business Media, 2013.

[27] Y. A. Kuznetsov and H. G. E. Meijer, *Numerical Bifurcation Analysis of Maps: From Theory to Software*. Cambridge University Press, 2019.

[28] G. Iooss, *Bifurcation of maps and applications*. Elsevier, 1979.

[29] J. D. Crawford, "Introduction to bifurcation theory," *Reviews of Modern Physics*, vol. 63, no. 4, p. 991, 1991.

[30] J. Carr, *Applications of centre manifold theory*, vol. 35. Springer Science & Business Media, 2012.

[31] W.-B. Zhang, *Discrete dynamical systems, bifurcations and chaos in economics*. elsevier, 2006.